

Vinyltrimethylsilane (VTMS) as a Probe of Chemical Reactivity of a TiCN Diffusion Barrier-Covered Silicon Surface

Laurent Pirolli and Andrew V. Teplyakov*

Department of Chemistry and Biochemistry, University of Delaware, Newark Delaware 19716

Received: October 15, 2005; In Final Form: December 27, 2005

This paper presents the first *molecular level* investigation of chemical reactivity of a surface of an amorphous diffusion barrier film deposited on a Si(100)-2 × 1 single crystal. Vinyltrimethylsilane (VTMS) is chosen as a probe molecule because of its chemical properties and because of its role as a ligand in a common copper deposition precursor, hexafluoroacetylacetonato-copper-vinyltrimethylsilane, (hfac)Cu(VTMS). The surface chemistry of vinyltrimethylsilane on titanium carbonitride-covered Si(100)-2 × 1 has been investigated using multiple internal reflection Fourier transform infrared spectroscopy (MIR-FTIR), Auger electron spectroscopy (AES), thermal desorption mass spectrometry, and computational analysis. On a film with nominal surface stoichiometry TiC_xN_y ($x \sim y \sim 1$) preannealed to 800 K, VTMS adsorbs molecularly at cryogenic temperatures even at submonolayer coverages; the major pathway for its temperature-programmed evolution is desorption. Adsorption at room temperature leads to chemisorption via a double-bond attachment. A set of computational models was designed to investigate the possible adsorption sites for a VTMS molecule on a TiCN-covered Si(100)-2 × 1 surface. A comparison of the computational predictions for a variety of possible adsorption sites with the results of thermal desorption and infrared measurements suggests that approximately 90% of the adsorbed VTMS is chemisorbed along the Ti–C bond while approximately 10% is chemisorbed on a Ti corner atom, the minority site of the surface. The Ti–N bond is not participating in the chemisorption process.

1. Introduction

Because of its uses in chemical deposition processes as a common ligand, vinyltrimethylsilane (VTMS) has received significant attention over the years. Its chemistry has been studied in detail on silicon,^{1,2} silicon oxide,³ copper,⁴ and other transition metals.⁵ The main goal of all these studies was to understand the chemical reactivity of all these materials with respect to VTMS so that the chemical deposition processes with organometallic compounds having VTMS as a ligand could be manipulated at the molecular level. One of the most widely used organometallic precursors for copper deposition is hexafluoroacetylacetonato-copper-vinyltrimethylsilane ((hfac)Cu(VTMS)).^{6,7} Thus, the studies of VTMS interaction with various supports prove mandatory to understand the copper deposition process. Interestingly, with the exception of copper-on-copper growth, all the previously studied systems can only be utilized as models for unusual applications of copper deposition methods, because in real applications, copper is almost never deposited directly on a semiconductor substrate. In the vast majority of devices, copper is separated from a semiconductor surface by a diffusion barrier material. One of the most prominent materials, possessing high thermal stability, good diffusion barrier properties, and low electrical resistivity is titanium nitride, TiN.^{8–12} This material can be deposited on a semiconductor substrate using such chemical vapor deposition precursors as dialkyl-amino derivatives (Ti[NR₂]₄, where R = Me, Et)^{13–28} and TiCl₄.^{8,29–32} used in combination with NH₃ and sometimes H₂; however, the latter method often presents significant problems associated with chlorine contamination and formation of NH₄Cl. The chemical and physical properties of TiN films can be controlled by

manipulating the carbon content, and in fact, titanium carbonitride films, TiC_xN_y, have been shown to have a set of very attractive physical properties, including better conformal filling than titanium nitride.^{33–35}

Despite the fact that to the best of our knowledge the studies of the chemistry of VTMS on surfaces of amorphous TiCN films have never been performed, this combination should provide an excellent benchmark for understanding the surface structure and reactivity of TiCN films. The presence of a double bond in a test molecule provides an ample set of bonding opportunities, and the presence of a bulky trimethylsilyl group affords a sensitive spectroscopic probe with respect to the specific environment of the surface reactive site. Simpler probe molecules, such as, for example, CO, O₂, and NH₃, described previously on various single-crystalline surfaces of titanium carbides and nitrides^{36–40} are not likely to yield any detailed information on the reactivity of somewhat complex surface reaction sites, including Ti–N or Ti–C, with a significant degree of inhomogeneity. On the other hand, the studies of VTMS on single crystals of titanium carbide and nitride materials are unlikely to provide a set of reasonable benchmarks for understanding its chemistry on an amorphous TiCN film. The very fact that the film is amorphous²¹ means that unlike on most single-crystal model surfaces, a specific reactive site cannot be isolated and analyzed explicitly. One more argument supporting the previous statement is the fact that in the computational studies of the reactions of titanium nitride and titanium carbide single-crystalline materials with CO and NH₃ the positions of the surface atoms could be fixed at their bulk values and nevertheless this simplification would yield an excellent agreement with the experimental measurements. As will be mentioned below, a similar approach in the studies of

* Corresponding author. Phone: (302) 831-1969. Fax: (302) 831-6335. E-mail: andrewt@udel.edu.

the amorphous TiCN reaction with VTMS would yield a lack of chemical reactivity while experimentally the reaction in question was shown to occur. Thus, a combination of VTMS as a probe molecule with the TiCN film prepared in situ will both provide an insight into the chemistry of VTMS on the TiCN surface and yield some information on the structure and properties of the surface itself.

This is the first study that starts with the diffusion barrier prepared on an ideal single-crystal Si(100)-2 \times 1 surface and follows the previously published procedures⁴¹ to maintain a controlled film thickness in every experiment. The deposition is done in an ultrahigh vacuum chamber. The exact structure of the surface of this film cannot be determined easily; however, knowing the overall stoichiometry of the surface and the structures of titanium carbide and titanium nitride single crystals, a simple computational model for TiCN reactive sites can be offered. On the basis of a strong chemisorption of VTMS on a surface of the TiCN films, several adsorption models will be discussed.

2. Methods

2.1. Experimental Methods. The two ultrahigh vacuum (UHV) chambers used in the studies described here are located at the University of Delaware. Both chambers have base pressure around 5×10^{-10} torr. They are both equipped for Auger electron spectroscopy, low-energy electron diffraction, and surface cleaning using an ion gun. One chamber is coupled to an infrared spectrometer (Nicolet, Magna 560) set up in a multiple internal reflection mode utilizing a liquid nitrogen cooled external MCT detector. A total of 2048 scans were collected in the infrared measurements with the resolution of 4 cm^{-1} . After the preparation of the TiCN-covered silicon crystal, the background spectrum was collected, then the appropriate dose of the compound of interest was introduced into the UHV chamber using a leak valve, and a brief annealing to the desired temperature was performed if needed. The spectrum was then collected at the same temperature as the background. The unshielded mass spectrometer (SRS 200) is used to determine the cleanliness of the dosing compounds in situ. The other UHV chamber was largely used for temperature-programmed desorption studies. It is equipped with a shielded differentially pumped mass spectrometer (Hidden Analytical) pumped by a dedicated ion pump. During the temperature-programmed desorption studies, the crystal was positioned ~ 2 mm away from a 2 mm aperture in the shield.

A $25 \times 20 \times 1$ mm trapezoidal sample of Si(100)-2 \times 1 with 45° beveled edges (Harrick Scientific) was used for the multiple internal reflection infrared spectroscopy studies. This sample, polished on both sides, was mounted on a manipulator capable of cooling the sample to 90 K with liquid nitrogen and heating it to above 1150 K using an e-beam heater (McAllister Technical Services). Another $1 \times 1 \text{ cm}^2$ silicon sample was cut from a Si(100) wafer (Semiconductor International) and mounted in a different chamber for temperature-programmed reaction/desorption (TPR/D) studies. This sample was polished on one Si(100) surface. The heating rate in the TPR/D studies was 2 K/s. The temperature range in this chamber was 130–1150 K.

The vinyltrimethylsilane (VTMS, Aldrich, 99%) was pre-purified by at least 10 freeze–pump–thaw cycles before introduction into the chamber. The purity of the compound was verified in situ by mass spectrometry, and the mass spectra obtained were compared with the available database mass spectrum of VTMS.⁴² Argon (Matheson, 99.999%) for surface cleaning was used without additional purification. Tetrakis-

(dimethylamino)-titanium (TDMAT, 99%, First Reaction) was transferred into a dosing vial with a valve in a nitrogen glovebox to avoid oxidation processes in air. It was subjected to multiple freeze–pump–thaw cycles before introduction into the vacuum chamber. The purity of this compound was verified in situ by mass spectrometry and by infrared analysis of a condensed multilayer at cryogenic temperatures.

The silicon crystals were prepared by sputtering with Ar^+ for 40 min at room temperature, followed by annealing for 20 min at 1150 K. This procedure leads to a clean and well-ordered Si(100)-2 \times 1 surface as confirmed by AES and LEED.

The deposition of the diffusion barrier layer was performed using a reaction of tetrakis-(dimethylamino)-titanium (TDMAT) at 600 K. A dose of 2000 L produced a layer approximately 5 nm thick with an rms roughness of 1–2 nm. The procedure for this deposition and the physical properties of the deposited film are described in ref 41. Larger exposures were used for the temperature-programmed desorption studies. Before the adsorption of the VTMS onto this surface, it was briefly annealed to 800 K. Throughout the paper this surface is referred to as the TiCN-covered Si(100)-2 \times 1 surface.

All exposures are reported in langmuirs (L), where $1 \text{ L} = 10^{-6} \text{ torr}\cdot\text{s}$. The pressures were not corrected for ion gauge sensitivity.

2.2. Computational Methods. Molecular orbital calculations⁴³ using density functional theory (DFT) were performed using the Gaussian 03 package.⁴⁴ The Becke three-parameter hybrid functional,^{45,46} combined with the Lee, Yang, and Parr (LYP) correlation functional, denoted B3LYP,⁴⁷ was employed in the calculations. The geometries of most model systems were optimized^{48–50} *without any symmetry constraints* using the LANL2DZ basis set.^{51–54} Then single-point calculations were performed using the 6-311+G(d,p) basis set.^{55–63} Simple models consisting of 20 atoms or fewer (with only one transition metal atom) were optimized using the 6-311+G(d,p) basis set. Harmonic vibrational frequencies were calculated analytically for each optimized structure. Zero-point vibrational energy (ZPVE) corrections were accounted for.

LANL2DZ basis set retains some of the outer-core functions when applied to third- and higher-period atoms. It has been successfully used before in our group to investigate the structural properties of Keggin structure polyoxometalates⁶⁴ and to investigate countercation and water bonding in Lindqvist structure polyoxometalates.⁶⁵ However, despite the fact that it is commonly used to investigate clustered systems, it is not often involved in vibrational studies of hydrocarbon fragments. Thus, in the studies presented here it is selectively compared with the 6-311+G(d,p) basis set, which is commonly used in investigations of adsorbed hydrocarbons and their fragments.

Several models of surface adsorption sites have been utilized in this study. $\text{Ti}_4\text{C}_2\text{N}_2$ and $\text{Ti}_2\text{N}_2\text{C}_4$ clusters with an even number of electrons were used with the assumption of a singlet electronic state, *vide infra*. The $\text{Ti}_4\text{C}_3\text{N}$ cluster with an odd number of electrons and assumed doublet electronic state was used to elucidate the electronic effects on surface binding of VTMS. Diatomic clusters, TiN (doublet) and TiC (singlet), were investigated to understand the effects of the adsorption geometry of VTMS on the appearance of the infrared spectra. In this case, the binding energy of VTMS bound to these diatomic clusters can only be used to illustrate the stability of gas-phase species rather than to understand the surface adsorption, but the infrared spectra predicted for these species are consistent with the species produced on more elaborate clusters. In some of the previous studies of titanium carbide and titanium nitride the *unterminated*

clusters of the type Ti_9X_9 , Ti_8X_8 , and $\text{Ti}_{13}\text{X}_{13}$, where $\text{X} = \text{N}$ or $\text{X} = \text{C}$, were successfully used to understand the electronic properties of the single-crystal carbide and nitride surfaces.^{36–38,66,67} However, in the above-mentioned studies,^{36–38,66,67} the positions of the atoms were fixed at bulk values and no surface reconstruction was explored. This approach provided excellent agreement with the experimental X-ray photoelectron spectroscopy and UV photoelectron spectroscopy data. It also proved valuable in understanding bonding of simple molecules, such as CO and NH_3 . For example, in the studies by Didziulis et al.³⁸ only one surface atom was primarily involved into chemisorption of CO or NH_3 and the fact that the atoms in the clusters representing the single-crystal surfaces were fixed bared no significant effects on the structures representing molecular adsorption on these crystals. In the studies presented here, the structures of all the clusters have been optimized before studying their interaction with VTMS. No geometrical restraints have been imposed to emulate the similarity of the clusters with the surface of the amorphous film rather than with single-crystalline materials. It should be mentioned that a single investigation of the interaction of a $\text{Ti}_{12}\text{C}_{12}$ cluster (similar to the ones used previously by Didziulis et al.³⁸) with all atomic positions fixed at the bulk values with a VTMS molecule was unsuccessful. It did not produce any stable structures for the VTMS molecule interacting with the atoms representing the (100) plane. This suggests that when multiple bonding geometries and bonding of several atoms of the adsorbed molecule to the surface are observed, the cluster models of the titanium carbide single-crystalline surfaces with fixed atomic coordinates should be treated with caution.

3. Experimental Results

The study of the reactions of the vinyltrimethylsilane (VTMS) with the $\text{Si}(100)\text{-}2 \times 1$ surface precovered with a titanium carbonitride diffusion barrier films has been conducted in two parts: cryogenic temperature adsorption and chemistry and room-temperature adsorption and chemistry.

3.1. Adsorption of VTMS on TiCN-Covered $\text{Si}(100)\text{-}2 \times 1$ at Cryogenic Temperature. The bonding and reactivity of VTMS with TiCN-covered $\text{Si}(100)$ have been explored using temperature-programmed desorption (TPD) and MIR-FTIR techniques starting at cryogenic temperatures of 100–130 K.

Figure 1 shows a series of TPD spectra for varying exposures of VTMS onto a TiCN-covered $\text{Si}(100)\text{-}2 \times 1$ surface at cryogenic temperature. The most intense peak in the VTMS mass spectrum, $m/z = 85$, was followed in this set of studies; however, other mass-to-charge ratios were also monitored to confirm that the desorbing molecule is indeed VTMS ($m/z = 59$, 100, etc., not shown here). The lowest temperature attainable in this experimental setup was 130 K, and the VTMS was dosed at this temperature. Similarly to our previous studies of VTMS on a clean $\text{Si}(100)\text{-}2 \times 1$,¹ the molecular desorption of VTMS was the major pathway for VTMS evolution on a TiCN-covered $\text{Si}(100)\text{-}2 \times 1$ surface. VTMS desorbs molecularly around 160 K even at the lowest exposures used. The plot of the TPD peak area as a function of VTMS exposure shown in the inset for Figure 1 suggests that the adsorption is reversible and no VTMS is decomposed on the TiCN-covered surface at cryogenic temperatures.

The infrared spectroscopy studies summarized in Figure 2 confirm the findings of the temperature-programmed desorption analysis. Even at an exposure of 1 L, the VTMS maintains its structure without noticeable chemisorption on a TiCN-covered $\text{Si}(100)\text{-}2 \times 1$ surface. The absorption bands at 1595 cm^{-1}

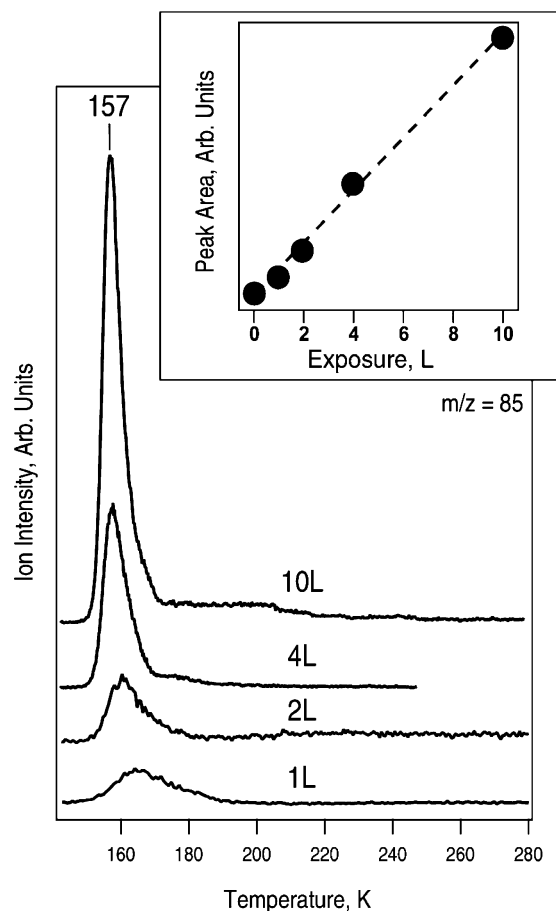


Figure 1. Temperature-programmed reaction/desorption studies of vinyltrimethylsilane (VTMS) adsorbed on a TiCN-covered $\text{Si}(100)\text{-}2 \times 1$ surface at cryogenic temperature (below 140 K); $m/z = 85$ was followed as a function of VTMS exposure. The inset shows the integrated peak areas as a function of the initial exposures.

($\nu_{\text{C}=\text{C}}$) and at 3048 cm^{-1} ($\nu_{\text{C}-\text{H}}$) confirm the integrity of the double bond. However, when compared to the spectrum of the same amount of VTMS adsorbed on a clean $\text{Si}(100)\text{-}2 \times 1$ surface at the same conditions as those depicted in Figure 2, it is clear that the infrared spectrum of this molecule on a TiCN-covered $\text{Si}(100)\text{-}2 \times 1$ surface exhibits a set of absorption bands between 2600 and 2800 cm^{-1} , which are not characteristic of the VTMS. A computational analysis of free VTMS has been performed to prove that these vibrations do not belong to the VTMS entity. Simulated spectra of a single VTMS molecule utilizing 6-311+G(d,p) and LANL2DZ basis sets are given in Figure 2. When appropriate scaling factors are used (0.96 for 6-311+G(d,p) and 0.947 for LANL2DZ), both approaches produce the vibrational spectrum of a VTMS molecule very well and none of the methods suggest the presence of the absorption signatures for the molecule around 2700 cm^{-1} . Of course, one major difference between the VTMS adsorption onto a clean $\text{Si}(100)\text{-}2 \times 1$ surface and its adsorption onto a TiCN-covered $\text{Si}(100)\text{-}2 \times 1$ surface is the presence of small amounts of TDMAT in the vacuum system after the diffusion barrier film deposition. When the spectrum of 1 L of VTMS on a TiCN-covered $\text{Si}(100)\text{-}2 \times 1$ surface is compared to that of TDMAT dosed onto the same surface intentionally at room temperature, the absorption bands at 1653 cm^{-1} , 2786 , 2826 , and 2859 cm^{-1} correlate well with the absorption features of TDMAT. These absorption bands represent only a small amount of the residual TDMAT in the UHV chamber, whose coverage can be estimated to be less than 5% of a monolayer based on our previous

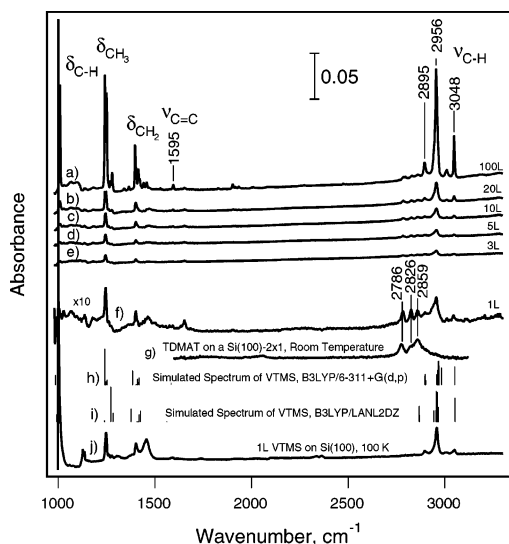


Figure 2. Summary of the MIR-FTIR studies of vinyltrimethylsilane (VTMS) on the TiCN-covered Si(100)-2 × 1 surface at a cryogenic temperature of 100 K for exposures of (a) 100 L, (b) 20 L, (c) 10 L, (d) 5 L, (e) 3 L, and (f) 1 L, as compared to (g) the spectrum of a saturation exposure of tetrakis-(dimethylamino) titanium, TDMAT, on a clean Si(100)-2 × 1 surface at room temperature, (j) a spectrum of 1 L of VTMS adsorbed on a Si(100)-2 × 1 surface at 100 K, and the simulated spectrum of a single VTMS molecule performed by (h) B3LYP/6-311+G(d,p) (scaling factor 0.96) and by (i) B3LYP/LANL2DZ (scaling factor 0.947).

studies,⁴¹ and comparison of the intensity of these peaks in the spectra of various exposures of VTMS (1, 3, 5, 10, 20, and 100 L) suggests that the amount of residual TDMAT, as expected, is independent of the VTMS exposure.

Thus, thermal desorption and infrared spectroscopy studies suggest that VTMS adsorbs molecularly on a TiCN-covered Si(100)-2 × 1 surface at cryogenic temperatures of 100–130 K. This adsorption is reversible and VTMS is easily released to the gas phase when the surface is heated.

3.2. Adsorption of VTMS on TiCN-Covered Si(100)-2 × 1 at Room Temperature and Its Reactions upon Surface Annealing. Figure 3 compares the room-temperature infrared studies of a saturation coverage of VTMS on (a) a TiCN-covered and (b) clean Si(100)-2 × 1 surface with a submonolayer coverage of VTMS adsorbed at 100 K (spectrum c) and with several computational models (vide infra). Most significantly, the absorption band at 3048 cm⁻¹, corresponding to the C–H stretching on a terminal C=C group, is absent in both room-temperature adsorption experiments. Thus, the double bond of VTMS is definitely participating in the reaction with the surface both on a clean Si(100)-2 × 1 and on a TiCN-covered Si(100)-2 × 1 sample.

Temperature-programmed reaction/desorption (TPR/D) studies shown in Figure 4 suggest that there are three main events upon heating of the saturated monolayer of VTMS adsorbed on a TiCN-covered Si(100)-2 × 1 surface at room temperature. The two features at 420 and 543 K correspond to the desorption of VTMS and to the evolution of propylene. The analysis of the mass spectra of both compounds and their comparison to the literature mass spectra⁴² suggest that the desorption process at 420 K corresponds to the evolution of VTMS, while at 543 K approximately 30% of the desorbing species is propylene. The third TPR/D peak at 622 K, that is only clearly distinguishable in an *m/z* = 41 trace in Figure 4d, was assigned to the decomposition products of the residual tetrakis-(dimethylamino)-titanium molecules interacting with the surface of the TiCN

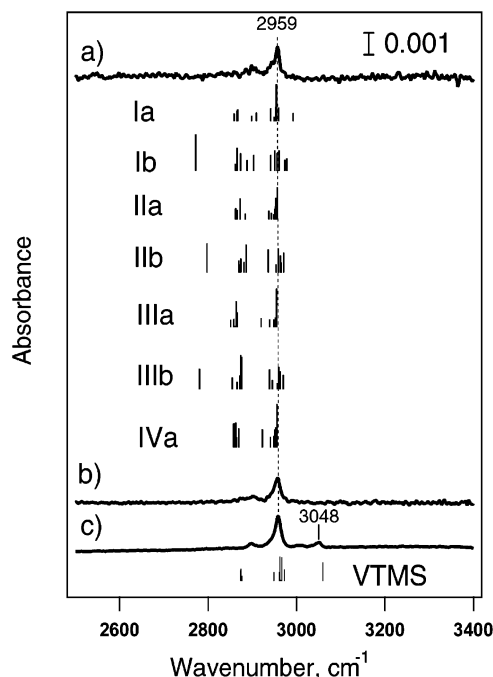


Figure 3. MIR-FTIR studies of (a) a saturation exposure of VTMS adsorbed on the TiCN-covered Si(100)-2 × 1 surface at 300 K, (b) a saturation exposure of VTMS adsorbed on a clean Si(100)-2 × 1 surface at 300 K, and (c) 1 L of VTMS adsorbed on a clean Si(100)-2 × 1 surface at 100 K compared to the simulated infrared spectra for the computational models indicated (see Table 1).

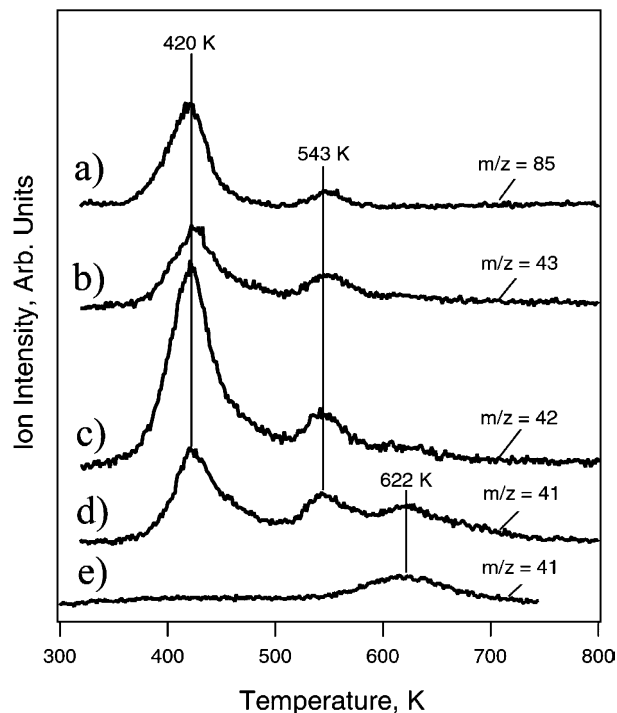


Figure 4. Thermal desorption studies of a saturation exposure of VTMS adsorbed on a TiCN-covered Si(100)-2 × 1 surface at room temperature tracing mass-to-charge ratios of (a) *m/z* = 85, (b) *m/z* = 43, (c) *m/z* = 42, (d) *m/z* = 41 as compared to (e) the blank experiment following *m/z* = 41 performed without exposing the TiCN-covered Si(100)-2 × 1 surface to VTMS.

film itself and is unrelated to the VTMS chemistry. In a blank experiment presented in Figure 4e, the TiCN-covered Si(100)-2 × 1 surface was prepared in exactly the same way as for the previous experiments but the thermal desorption trace was collected without dosing VTMS. The appearance of the

desorption feature around 622 K coincides with the same desorption feature present in the thermal desorption studies of VTMS, thus confirming that it originates from the residual TDMAT reaction with the TiCN film. Despite the fact that the surface is briefly annealed to 800 K before each experiment, the 622 K feature persists suggesting that even though the amount of residual TDMAT present in the vacuum chamber during the annealing/cooling cycle is very small, it still can adsorb on a reactive surface of titanium carbonitride.

4. Discussion

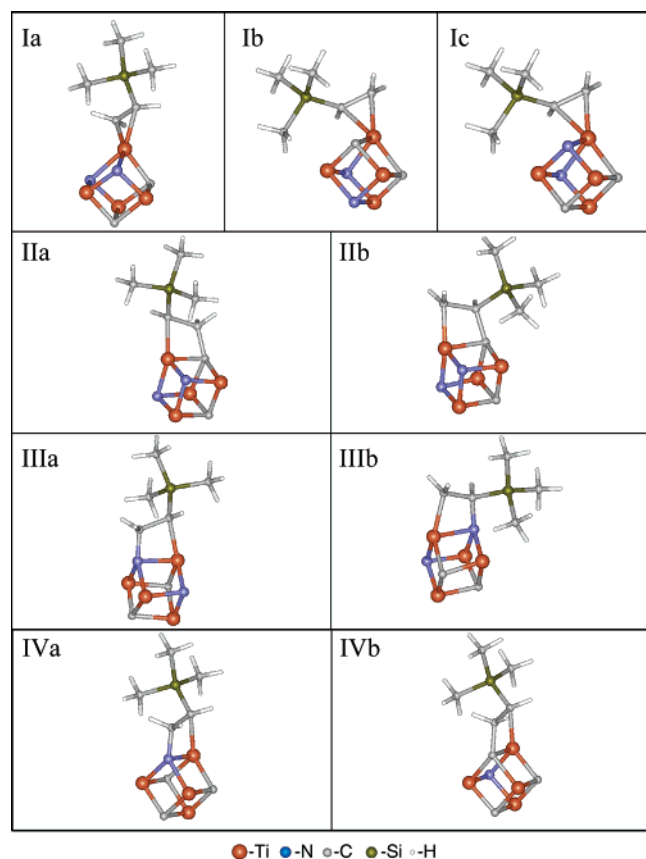
To understand and explain the energetics of adsorption and surface reactions of VTMS on a TiCN-covered Si(100)-2 \times 1 film, first the analysis of the cryogenic adsorption data should be performed. Similarly to the VTMS adsorption on a clean Si(100)-2 \times 1 surface,¹ the activation energy calculated for the 164 K feature (at a low surface coverage of 1 L the desorption can be assumed to follow the first order) yields a value of 42.1 kJ/mol when the Redhead method with a preexponential factor of 10^{13} s^{-1} is used.⁶⁸ This is characteristic of a physisorbed molecule and is remarkably similar to the ΔH of sublimation for VTMS, $\Delta H_s = 40.7 \text{ kJ/mol}$, which can be calculated based on the ΔH of fusion, $\Delta H_{\text{fusion}} = 7.6 \text{ kJ/mol}$ ⁶⁹ and the ΔH of evaporation, $\Delta H_{\text{vap}} = 33.1 \text{ kJ/mol}$.⁷⁰ Thus, the chemisorption barrier for VTMS on the TiCN-covered Si(100)-2 \times 1 surface should be higher than 42.1 kJ/mol, since the temperature-programmed desorption studies confirm the absence of any surface reactions other than molecular desorption. It should be noted that the activation barrier for chemisorption of such molecules as nitromethane, nitroethane, and nitrobenzene on Si(100)-2 \times 1,^{71,72} is observed experimentally, while in all the computational studies of these organic molecules with a silicon surface the chemisorption barrier is generally very small. Several major factors that play a role in this discrepancy have been outlined in ref 72.

Once the chemisorption barrier, however small, is overcome by a large exposure of VTMS onto a TiCN-covered Si(100)-2 \times 1 surface at room temperature, the analysis of the chemisorption products can be performed with the help of a computational approach. The surfaces of single-crystal titanium carbide and nitride materials have been attracting serious attention for the past few years, largely due to a set of great properties that these materials possess.⁷³ The high hardness and high melting point warrant the use of these materials as wear-resistant coatings. In addition, their unusual chemical properties and the similarity of their surface chemistry to that of precious materials^{74–76} pointed to the use of titanium carbides and nitrides as catalysts. However, only a few theoretical investigations relate the computational models with the actual experiments. Some of this work has been reviewed in a thorough investigation of CO and NH₃ bonding to the clusters representing various single-crystal faces of titanium carbide and titanium nitride.³⁸ This reference also provides an excellent reasoning behind choosing singlet or doublet electronic states for the models describing titanium carbide and nitride surfaces, respectively. In that study the Ti–C and Ti–N bonds and all the angles were fixed at the bulk values, and the obtained data correlated well with the experimental XPS and UPS spectra.³⁸ However, to the best of our knowledge there are no computational studies of the TiCN surface to date. In addition, in a contrast with the single-crystal studies, the amorphous nature of the TiCN films discussed in this paper precludes the possibility of fixing the positions of Ti, N, and C atoms to the bulk values or even imposing a set of geometrical constraints as has been done with carbide and

nitride single-crystal surfaces.³⁸ The surface of the TiCN film has approximately the same overall stoichiometry as that of the bulk, TiC_xN_y, where $x \sim y \sim 1$, and in the previous studies it was concluded that most of nitrogen atoms are bound to titanium, while carbon atoms are either bound to titanium or can be represented as “organic carbon”.^{33,77} The formation of a covalent bond between VTMS molecules and “organic carbon” is highly unlikely, regardless of the exact nature of this material, which is still debated. Its chemical properties should be similar to either hydrocarbons or graphite. In the case of hydrocarbons, saturated or not, the reaction with VTMS would have a very large barrier, essentially insurmountable at room temperature. The same statement seems to be true for graphite, based on the studies of the highly oriented pyrolytic graphite.^{78–80} Our own transmission electron microscopy investigation of the TiCN films deposited in ultrahigh vacuum conditions onto a clean and well-ordered Si(100)-2 \times 1 surface suggest that the films are indeed amorphous with a large number of small, 5–8 nm in diameter, crystallites. The structure of these films depends on the thickness.⁸¹ At the same time, for the studies presented here, with film thickness below 10 nm, the structure of the films is the same as the one postulated previously.^{33,77} In other words, the surface of this film corresponds to the nominal Ti-to-C-to-N ratio of 1-to-1-to-1, while a significant amount of carbon is supposedly represented by “organic carbon”, unreactive with respect to our probe molecule, VTMS. The exact structure of the surface of the TiCN film is not known; however, its most crucial features can be represented by a reasonably simple model.

The choice of the appropriate computational model is a crucial one, and it is especially difficult if the exact structure of the surface studied is not well defined. The surface of the TiCN film described here may be based on a structure of titanium nitride or carbide single-crystalline particles with some amount of one nonmetal replaced by the other. As mentioned above, according to our recent studies, the nature of TiCN film can be best described as nanocrystalline particles imbedded into the amorphous material surrounding them; a careful examination of these nanocrystallites suggests that they do indeed resemble the titanium carbide and nitride and that other possibilities, such as, for example, structural similarities to metcars,^{82,83} can be ruled out. Thus, the model needed should represent the structure of, for example, the titanium nitride nanocrystallites with some atoms replaced by carbon. The majority of the models used in these studies will have a general stoichiometry of TiC_{1–x}N_x. There is seemingly a contradiction arising from the fact that the stoichiometry of the model used is different from the overall stoichiometry of the film; however, taking into account the presence of the extra “organic carbon” alleviates this contradiction. Even after all these simplifications, the exact nature of the computational cluster model used here can still be very complicated. Interestingly, if one uses a small nearly cubic cluster, Ti₄C₂N₂, this model represents all the possible types of binding sites, even though in a real system, the exact environment of these binding sites can vary. Since no metallic titanium was observed based on the XPS data,⁸¹ the film in question should have Ti–C and Ti–N binding sites for a double bond of VTMS. Also, the interaction of VTMS with a single Ti corner atom, similar to the representative surface sites on (100) faces of titanium carbide and nitride,³⁸ should be considered. The Ti₄C₂N₂ model has all these chemisorption sites that can be tested by reacting with a VTMS molecule. This oversimplified model was also modified to have only one nitrogen present, Ti₄C₃N, and also to represent a Ti₂N₂ entity imbedded into the

TABLE 1: Computational Models Used to Describe VTMS Adsorption onto an Amorphous TiCN Film: I–III—Adsorption on a $\text{Ti}_4\text{C}_2\text{N}_2$ Cluster with a Singlet Ground State; IV—Adsorption on a $\text{Ti}_4\text{C}_3\text{N}$ Cluster with a Doublet Ground State



carbon structure, $\text{Ti}_2\text{N}_2\text{C}_4$. All these models provide a set of similar results when tested for reacting with VTMS, which seems to suggest that the surface chemistry of TiCN film depends largely on the local electronic and geometric structure rather than the extended ensemble effects of surface sites.

A possibility of an adsorption barrier has only been investigated for structure Ia presented in Table 1, and the application of the B3LYP/LANL2DZ approach did not yield any energy barrier upon addition of the VTMS molecule to the $\text{Ti}_4\text{C}_2\text{N}_2$ cluster. Interestingly, our previous ex situ near-edge X-ray absorption fine structure studies⁴¹ suggest that the surfaces of the films produced by TDMAT deposition contain both Ti^{2+} and Ti^{4+} , with the latter one dominating on the oxidized surfaces, where a significant concentration of oxygen leads to the formation of TiO_2 . Thus, the exact oxidation state of Ti in the clusters used here can be a subject of a separate investigation.

The structures based on the VTMS interaction with the $\text{Ti}_4\text{C}_2\text{N}_2$ and $\text{Ti}_4\text{C}_3\text{N}$ (vide infra) models optimized using the LANL2DZ basis set are presented in Table 1. Their energies (with and without the zero-point vibrational energy, ZPVE), as well as the single-point energies computed by using the 6-311+G(d,p) basis set, are given in Table 2, as compared to the energy of the free VTMS molecule and an optimized $\text{Ti}_4\text{C}_2\text{N}_2$ or $\text{Ti}_4\text{C}_3\text{N}$ structures. No imaginary frequencies were recorded for the optimized structures (see the Supporting Information) confirming the true minima.

The activation energy for desorption based on the Redhead method⁶⁸ applied to the 420 and 543 K desorption peaks assuming a first-order desorption process with a heating rate of

TABLE 2: Summary of the Computational Studies Used to Describe VTMS Adsorption onto an Amorphous TiCN Film^a

	B3LYP/LANL2DZ		
	relative electronic energy	relative electronic energy + ZPVE	single-point calculation: relative electronic energy: B3LYP/6-311+G(d,p)//B3LYP/LANL2DZ
VTMS + $\text{Ti}_4\text{C}_2\text{N}_2$	0.0	0.0	0.0
Ia	−170.2	−167.6	−140.5
Ib	−166.1	−161.6	−135.5
Ic	−176.9	−172.2	
IIa	−135.3	−131.6	−109.9
IIb	−125.8	−123.6	−94.6
IIIa	−46.2	−40.5	−24.6
IIIb	−39.0	−34.5	−2.6
VTMS + $\text{Ti}_4\text{C}_3\text{N}$	0.0	0.0	
IVa	−33.8	−29.6	
IVb	−83.3	−84.5	

^a The energies are given in kJ/mol as compared to the energy of VTMS and $\text{Ti}_4\text{C}_2\text{N}_2$ (for structures I–III) or $\text{Ti}_4\text{C}_3\text{N}$ (for structure IV) optimized by B3LYP/LANL2DZ. Single-point calculations using B3LYP/6-311+G(d,p) are given with respect to a single-point B3LYP/6-311+G(d,p) calculation for $\text{Ti}_4\text{C}_2\text{N}_2$ and a fully optimized structure of VTMS using the same basis set.

TABLE 3: Activation Energies, E_a , in kJ/mol Obtained by the Redhead Method with Various Preexponential Factors, ν , from Temperature-Programmed Desorption Studies with a 2 K/s Heating Rate

peak temp, K	$\nu = 10^{13} \text{ s}^{-1}$	$\nu = 10^{14} \text{ s}^{-1}$	$\nu = 10^{15} \text{ s}^{-1}$
420	110.5	118.5	126.6
543	144.0	154.4	164.8

2 K/s are given in Table 3 for three different preexponential factors: 10^{13} , 10^{14} , and 10^{15} s^{-1} .

The differences between structures Ia and Ic in Table 1 are caused by the asymmetry of the VTMS molecule. These models would be identical if the molecule reacted with the TiC_2N_2 cluster were ethylene. However, in model Ia, the trimethylsilyl group is directed away from the plane formed by two nitrogen atoms and one carbon atom bonded to the Ti atom representing the corner site. In model Ic, the trimethylsilyl group is directed toward this plane. The differences between the models of type I as compared to those of type II or type III are much more obvious and are simply based on the local binding site: corner Ti versus Ti–C versus Ti–N. While it is difficult to argue that the energy differences predicted, for example, for structures Ia and Ib, are significant enough—especially in that the exact types of the adsorption sites on a surface of the TiCN film are not known—it is definitely true that the energies computed for structures I(a or b) and II(a or b) line up very nicely with the energies calculated based on the thermal desorption experiments. Thus, for the type of model considered, the binding of VTMS along the Ti–N bond is by far the weakest. At the same time, the energies of binding along the TiC bond or on the Ti corner atom are remarkably similar to the experimental values.

Of course, electronic structure may have a pronounced effect on the binding energies. It was argued by Didziulis et al.³⁸ that while a singlet ground state used in clusters describing the electronic structure of the TiC surface works really well, the TiN surface represented by the cluster models with the odd number of electrons should be best described by a spin multiplicity of 2. Thus, a different model, $\text{Ti}_4\text{C}_3\text{N}$ with a doublet electronic state, was used to explore the effect of the surface electronic state on the binding energies of VTMS to form the structures IVa and IVb depicted in Table 1. Since the energy differences of the isomers produced because of the asymmetry

of a double bond in VTMS proved to be small by computational methods, only one representative isomer was chosen for investigating VTMS interaction with Ti–N bond and Ti–C bond. The results of both calculations (structures IVa and IVb) agree with the results produced by using the $\text{Ti}_4\text{C}_2\text{N}_2$ model (structures IIIa and IIa, respectively), as evidenced by the results in Table 2. Of course, in case of structures IVa and IVb the energy was compared to the energy of a free VTMS and an optimized $\text{Ti}_4\text{C}_3\text{N}$ cluster. From this analysis, it can be deduced that VTMS desorbing at 420 K corresponds to the VTMS bonded to a Ti–C bond, while the peak at 543 K represents a VTMS entity bonded to the corner Ti atom.

While structures Ia and Ib are similar energetically, the corresponding infrared signatures differ significantly. The same is true for structures IIa and IIb. The comparison in Figure 3 suggests that structure Ib would have an absorption feature of significant intensity around 2800 cm^{-1} , corresponding to the softened, red-shifted, $\nu_{\text{sym}}(\text{CH}_3)$ mode. However, in a structure Ia, where the trimethylsilyl group is directed away from the surface, there is no observable softening of the $\nu_{\text{sym}}(\text{CH}_3)$ mode. Similar effects are observed upon comparing structures IIa and IIb as well as structures IIIa and IIIb. Thus, on the basis of the vibrational spectra comparison, structures Ib, IIb, and IIIb can be ruled out as the major species present on the surface of TiCN films. Interestingly, the electronic state of the surface does not show any significant effects on the vibrational signature of the model species, as evident by the comparison of VTMS adsorbed along the Ti–N bond in structures IIIa and IVa or along the Ti–C bond in structures IIa and IVb. The infrared spectra for these pairs are very similar. A spectrum for a model IVa is given in Figure 3 (see the Supporting Information for a complete set of spectra over the full spectral range).

Obviously, the type of analysis presented in the previous paragraph is always attractive, and it is often efficient in well-defined systems. However, in the case of an amorphous material such as TiCN, there is definitely a distribution of adsorption sites available for interaction with a probe molecule, and the effects of the mode softening observed in one model may not be observed in another. To investigate the effects of adsorption environment on the vibrational spectra of the hydrocarbon fragment, a set of diatomic molecules with VTMS adsorbed on them was investigated. The interaction of diatomic clusters of TiN (spin multiplicity 2) and TiC (spin multiplicity 1) with VTMS was analyzed for the models presented in Table 4 and compared with a VTMS molecule adsorbed on a single atom of titanium.

The energies of formation of all these compounds from VTMS and a diatomic or monatomic model may not and most likely do not represent anything comparable with the surface binding of VTMS. However, for the purposes of comparison of the vibrational spectra of the produced entities they are perfectly acceptable.

A summary of these investigations is given in Figure 5. It is very clear that the structure VII with VTMS bonded to a single Ti atom produces an infrared spectrum that is almost exactly the same as in structure Ia. The spectra of species Va, Vb, VIa, and VIb line up very nicely with the predicted spectra of structures IIa, IIb, IIIa, and IIIb, respectively. There is some difference in the exact position of the absorption band corresponding to the softened $\nu_{\text{sym}}(\text{CH}_3)$ mode; however, if the Ti–N (or Ti–C) distance in a diatomic cluster is fixed at the bulk value (2.160 \AA for Ti–C and 2.140 \AA for Ti–N³⁸) the corresponding spectra presented in Figure 5 for Vb (Ti–N fixed) and VIb (Ti–C fixed) are very similar to the ones of IIb and

TABLE 4: Computational Models Used to Describe VTMS Adsorption onto an Amorphous TiCN Film^a

Va	Vb
VIa	VIb
VII	

● -Ti ● -N ● -C ● -Si ● -H

^a B3LYP/6-311+G(d,p) was used to fully optimize all these structures.

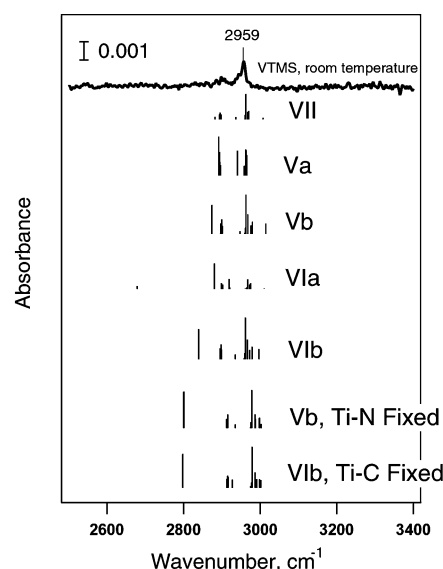


Figure 5. Comparison of the MIR-FTIR studies of a saturation exposure of VTMS adsorbed on the TiCN-covered Si(100)- 2×1 surface at 300 K with a set of simulated spectra generated for the computational models in Table 4. A scaling factor of 0.96 is used for this comparison.

IIIb. It can be concluded that the softening of the $\nu_{\text{sym}}(\text{CH}_3)$ in one of the methyl groups in a trimethylsilyl fragment is very sensitive to the distance between the carbon of the vinyl group that it is connected to and the surface. In other words, on a TiCN surface, if the trimethylsilyl group of VTMS is bonded to the vinylic carbon connected to C or N (shorter distance to the surface) significant softening of this mode is observed. However, if the corresponding vinylic carbon is attached to Ti (longer distance to the surface), no softening is observed. While softened modes in experimental vibrational spectra can be often represented by broad and difficult to detect absorption features, the signal-to-noise in the experiments presented here allows us

TABLE 5: Comparison of the Experimental Activation Energy Differences and Theoretical Predictions^a

ΔE_a , $\nu = 10^{13}$, s ⁻¹	33.5
ΔE_a , $\nu = 10^{14}$, s ⁻¹	35.9
ΔE_a , $\nu = 10^{15}$, s ⁻¹	38.2
electronic energy difference between structures IIa and Ia, B3LYP/LANL2DZ	34.9
(electronic energy + ZPVE) difference between structures IIa and Ia, B3LYP/LANL2DZ	36.0
electronic energy difference between structures IIa and Ia, single-point calculation: B3LYP/6-311+G(d,p)//B3LYP/LANL2DZ	30.5

^a Energies are given in kJ/mol.

to safely rule out a number of structures where significant mode softening is expected.

To summarize all these computational investigations, it is clear that the species present on a surface of TiCN film are of the type of Ia and IIa. The species based on VTMS reaction with the TiN bonding site can be ruled out because of their low binding energy, and species of the type of Ib and IIb can also be eliminated based on the comparison of the predicted and observed infrared spectra.

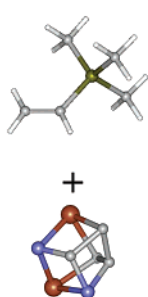
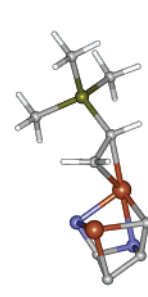
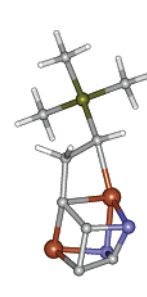
It should be noted that there is a significantly larger number of isomers available for investigation compared to the ones chosen here. For example, structure Ib is produced by attaching the VTMS molecule to the titanium corner atom connected to *one nitrogen* and *two carbon* atoms. A similar structure, Ic, shown in Table 1, could also be produced by reacting VTMS with the titanium corner atom connected to *one carbon* and *two nitrogens*. Energetically, structures Ib and Ic are similar, as evidenced in Table 2. Infrared spectra of these two structures are almost identical (see the Supporting Information for exact comparison). Thus, the effects of the second neighbors are not expected to play any significant role in this investigation. They do, however, leave some room for further analysis when the reactions of larger molecules and fragments with the surface of the TiCN film are considered.

Species Ia and IIa are likely present on the surface simultaneously at room temperature. On the basis of the temperature-programmed desorption studies, the energetic difference between Ia and IIa is around 35–40 kJ/mol and approximately 90% of the surface adsorption sites lead to the formation of the species of the type IIa, while the rest of the adsorbed sites produce VTMS bonded to the corner Ti atom. In fact, the binding energy of VTMS to the titanium corner atom sites is so high that upon thermal annealing, approximately 30% of these surface adsorbates decompose.

Table 5 presents a comparison of the experimentally observed difference between two majority desorption processes compared to all the computational energy differences between structures Ia and IIa calculated using different basis sets, with or without inclusion of the zero-point vibrational energy correction. The computational prediction agrees with the experimental observation extremely well.

Finally, to understand the effects of the stoichiometry on the VTMS binding to the titanium carbonitride and to confirm the generality of the models chosen, a set of selected studies of VTMS reaction with the Ti₂N₂ entity imbedded in a carbon frame were performed using B3LYP/6-311+G(d,p). As summarized in Table 6, the stability of the products of VTMS reaction with the Ti₂N₂C₄ cluster is completely consistent with the studies of other clusters described here. VTMS chemisorbed

TABLE 6: Computational Studies of VTMS Interaction with a Ti₂N₂C₄ Cluster Model with a Singlet Ground State^a

VIII	VIIIa	VIIIb
		
0 kJ/mol	-163.1 kJ/mol	-119.0 kJ/mol

^a B3LYP/6-311+G(d,p) was used to fully optimize all these structures.

on the Ti₂N₂C₄ cluster along the Ti–C bond is –119.0 kJ/mol more stable than the reactants. This number is in an excellent agreement with the stability of an equivalent structure based on a Ti₄C₂N₂ cluster, IIa. The VTMS molecule chemisorbed on a corner atom of the Ti₂N₂C₄ cluster also shows a great similarity to its equivalent structure, Ia. Its stability is –163.1 kJ/mol as compared to –170.2 kJ/mol for structure Ia.

Thus, it appears that the reactivity of the specific surface sites on the amorphous titanium carbonitride film with respect to a VTMS probe molecule depends largely on the electronic and geometric structure of the localized reactive site and not on the overall structure of the ensemble of atoms as represented by a variety of cluster models investigated here.

5. Conclusions

This is the first, to the best of our knowledge, molecular level investigation of the amorphous TiCN film deposited onto a clean single-crystal Si(100)-2 × 1 surface in ultrahigh vacuum conditions and compared with the computational data. On the basis of this integrated approach, the bonding of VTMS molecules to the thin film surface is suggested to occur via reaction of the double bond of VTMS with the surface Ti–C sites and with the corner Ti atoms available on a surface of this film. Much lower binding energy between VTMS and the Ti–N adsorption site as compared to the Ti and Ti–C sites observed in computational investigation suggests that there may still be nitrogen sites available on this surface even after its saturation with VTMS.

On a Ti corner site, VTMS is adsorbed in such a way that the trimethylsilyl group is directed away from the surface (Ia); on the Ti–C site, VTMS is adsorbed with the CH₂ entity of the vinyl group attached to carbon atom and with the CHSi(CH₃)₃ attached to titanium. Understanding these binding geometries will help in designing more efficient surface deposition pathways and will allow further computational investigations of the amorphous materials such as TiCN films.

Acknowledgment. Acknowledgment is made to the National Science Foundation (CHE-0313803) for the support of this research. A.V.T. also thanks Professor Douglas J. Doren, Mr. Jeffrey Frey, and Dr. Olga Dmitrenko (Department of Chemistry and Biochemistry, University of Delaware) for useful discussions.

Supporting Information Available: Cartesian coordinates and IR frequencies; complete ref 44. This material is available free of charge via the Internet at <http://pubs.acs.org>.

References and Notes

- Pirulli, L.; Teplakov, A. V. *J. Phys. Chem. B* **2005**, *109* (17), 8462–8468.
- Andersohn, L.; Kochanski, G. P.; Norman, J. A. T.; Hinch, B. J. *J. Vac. Sci. Technol., B* **1996**, *14* (2), 1032–1037.
- Dubois, L. H.; Zegarski, B. R. *J. Electrochem. Soc.* **1992**, *139*, 3295.
- Schulz, D. L.; Curtis, C. J.; Ginley, D. S. *Electrochem. Solid-State Lett.* **2001**, *4* (8), C58–C61.
- Gentle, T. M.; Grassian, V. H.; Klarup, D. G.; Muetterties, E. L. *J. Am. Chem. Soc.* **1983**, *105* (22), 6766–6767.
- Hampden-Smith, M. J.; Kostas, T. T. *Polyhedron* **1995**, *14* (6), 699–732.
- Murarka, S. P. *Mater. Sci. Eng.* **1997**, *R19*, 87–151.
- Chourasia, A. R.; Chopra, D. R. *Thin Solid Films* **1995**, *266*, 298–301.
- Ducroquet, F.; Achard, H.; Coudert, F.; Prévitali, B.; Lugand, J.-F.; Ulmer, L.; Farjot, T.; Gobil, Y.; Heitzmann, M.; Tedesco, S.; Nier, M.-E.; Deleonibus, S. *IEEE Trans. Electron Devices* **2001**, *48* (8), 1816–1821.
- Yagishita, A.; Saito, T.; Nakajima, K.; Inumiya, S.; Matsuo, K. *IEEE Trans. Electron Devices* **2001**, *48* (8), 1604–1611.
- Lau, J. T.; Prybyla, J. A.; Theiss, S. K. *Appl. Phys. Lett.* **2000**, *76* (2), 164–166.
- Motte, P.; Proust, M.; Torres, J.; Gobil, Y.; Morand, Y.; Palleau, J.; Pantel, R.; Juhel, M. *Microelectron. Eng.* **2000**, *50*, 369–374.
- Prybyla, J. A.; Chiang, C.-M.; Dubois, L. H. *Mater. Res. Soc. Symp. Proc.* **1993**, *282*, 281–292.
- Prybyla, J. A.; Chiang, C.-M.; Dubois, L. H. *J. Electrochem. Soc.* **1993**, *140* (9), 2695–2702.
- Weiller, B. H. *Mater. Res. Soc. Symp. Proc.* **1993**, *282*, 605–610.
- Dubois, L. H. *Polyhedron* **1994**, *13* (8), 1329–1336.
- Corneille, J. S.; Chen, P. J.; Truong, C. M.; Oh, W. S.; Goodman, D. W. *J. Vac. Sci. Technol., A* **1995**, *13* (3), 1116–1120.
- Paranjpe, A.; IslamRaja, M. *J. Vac. Sci. Technol., B* **1995**, *13* (5), 2105–2114.
- Kim, D.-H.; Cho, S.-L.; Kim, K.-B.; Kim, J. J.; Park, J. W.; Kim, J. J. *Appl. Phys. Lett.* **1996**, *69* (27), 4182–4184.
- Shin, H.-K.; Shin, H.-J.; Lee, J.-G.; Kang, S.-W.; Ahn, B.-T. *Chem. Mater.* **1997**, *9*, 76–80.
- Kim, D.-H.; Lim, G. T.; Kim, S.-K.; Park, J. W.; Lee, J.-G. *J. Vac. Sci. Technol., B* **1999**, *15* (5), 2197–2203.
- Min, J.-S.; Park, H.-S.; Kang, S.-W. *Appl. Phys. Lett.* **1999**, *75* (11), 1521–1523.
- Kim, D.-J.; Jung, Y.-B.; Lee, M.-B.; Lee, Y.-H.; Lee, J.-H.; Lee, J.-H. *Thin Solid Films* **2000**, *372*, 276–283.
- Liu, X.; Wu, Z.; Cai, H.; Yang, Y.; Chen, T.; Vallet, C. E.; Zuh, R. A.; Beach, D. B.; Peng, Z.-H.; Wu, Y.-D.; Concollino, T. E.; Rheingold, A. L.; Xue, Z. *J. Am. Chem. Soc.* **2001**, *123*, 8011–8021.
- Gross, J. B.; Schlegel, H. B. *Chem. Phys. Lett.* **2001**, *340*, 343–347.
- Okada, L. A.; George, S. M. *Appl. Surf. Sci.* **1999**, *137*, 113–124.
- Lee, J.-G.; Kim, J.-H.; Shin, H.-K.; Park, S.-J.; Yun, D.-J.; Kim, G.-H. *Mater. Res. Soc. Symp. Proc.* **1996**, *427*, 371–376.
- Norton, E. T., Jr.; Amato-Wierda, C. C. *Electrochem. Soc. Proc.* **2001**, *2001*–13, 9–16.
- Buiting, M. J.; Otterloo, A. F. *J. Electrochem. Soc.* **1992**, *139* (9), 2580–2584.
- Ritala, M.; Leskelä, M.; Rauhala, E.; Haussalo, P. *J. Electrochem. Soc.* **1995**, *140* (8), 2731–2737.
- Perry, A. J. *Surf. Coat. Technol.* **2000**, *132*, 21–35.
- Umanski, S. Y.; Novoselov, K. P.; Minushev, A. K.; Siodmiak, M.; Frenking, G.; Korkin, A. A. *J. Comput. Chem.* **2001**, *22* (13), 1366–1376.
- Eizenberg, M.; Littau, K.; Ghanayem, S.; Mark, A.; Maeda, Y.; Chang, M.; Sinha, A. K. *Appl. Phys. Lett.* **1994**, *65* (19), 2416–2418.
- Fuentes, G. G.; Elizalde, E.; Sanz, J. M. *J. Appl. Phys.* **2001**, *90* (6), 2737–2743.
- Kozłowski, J.; Markowski, J.; Prajzner, A.; Zdanowski, J. *Surf. Coat. Technol.* **1998**, *98*, 1440–1443.
- Didziulis, S. V.; Frantz, P.; Fernandez-Torres, L. C.; Guenard, R. L.; El-bjeirami, O.; Perry, S. S. *J. Chem. Phys.* **2001**, *105*, 5196–5209.
- Fernández-Torres, L. C.; Perry, S. S.; Didziulis, S. V.; Frantz, P. *Surf. Sci.* **2002**, *511*, 121–132.
- Didziulis, S. V.; Butcher, K. D.; Perry, S. S. *Inorg. Chem.* **2003**, *42* (24), 7766–7781.
- Liu, P.; Rodriguez, J. A. *J. Chem. Phys.* **2004**, *120*, 5414–5423.
- Rodriguez, J. A.; Liu, P.; Dvorak, J.; Jirsak, T.; Gomes, J.; Takahashi, Y.; Nakamura, K. *J. Chem. Phys.* **2004**, *121*, 465–474.
- Bocharov, S.; Zhang, Z.; Beebe, T. P., Jr.; Teplakov, A. V. *Thin Solid Films* **2005**, *471*, 159–165.
- NIST Chemistry Webbook. <http://webbook.nist.gov/chemistry/> (April 2003).
- Hehre, W. J.; Radom, L.; Schleyer, P. v. R.; Pople, J. A. *Ab Initio Molecular Orbital Theory*; Wiley: New York, 1986.
- Frisch, M. J. T.; et al. *Gaussian 03*, revision C.02; Gaussian, Inc.: Wallingford, CT, 2004.
- Becke, A. D. *Phys. Rev. A* **1988**, *38* (6), 3098–3100.
- Becke, A. D. *J. Chem. Phys.* **1993**, *98* (7), 5648–5652.
- Stevens, P. J.; Devlin, F. J.; Chabalowski, C. F.; Frisch, M. J. *J. Phys. Chem.* **1994**, *98* (45), 11623–11627.
- Schlegel, H. B. *J. Comput. Chem.* **1982**, *3* (2), 214–218.
- Schlegel, H. B. *Adv. Chem. Phys.* **1987**, *67* (Part 1), 249–286.
- Schlegel, H. B. In *Modern Electronic Structure Theory*; Yarkony, D. R., Ed.; World Scientific: Singapore, 1995; p 459.
- Dunning, T. H., Jr.; Hay, P. J. In *Modern Theoretical Chemistry*; Schaefer, H. F., III, Ed.; Plenum: New York, 1976; Vol. 3, pp 1–28.
- Hay, P. J.; Wadt, W. R. *J. Chem. Phys.* **1985**, *82*, 270.
- Wadt, W. R.; Hay, P. J. *J. Chem. Phys.* **1985**, *82*, 284.
- Hay, P. J.; Wadt, W. R. *J. Chem. Phys.* **1985**, *82*, 299.
- McLean, A. D.; Chandler, G. S. *J. Chem. Phys.* **1980**, *72*, 5639.
- Krishnan, R.; Binkley, J. S.; Seeger, R.; Pople, J. A. *J. Chem. Phys.* **1980**, *72*, 650.
- Blaudeau, J.-P.; McGrath, M. P.; Curtiss, L. A.; Radom, L. *J. Chem. Phys.* **1997**, *107*, 5016.
- Wachters, A. J. H. *J. Chem. Phys.* **1970**, *52*, 1033.
- Hay, P. J. *J. Chem. Phys.* **1977**, *66*, 4377.
- Raghavachari, K.; Trucks, G. W. *J. Chem. Phys.* **1989**, *91*, 1206.
- Binning, R. C., Jr.; Curtiss, L. A. *J. Comput. Chem.* **1990**, *11*, 1206.
- Curtiss, L. A.; McGrath, M. P.; Blaudeau, J.-P.; Davis, N. E.; Binning, R. C., Jr.; Radom, L. *J. Chem. Phys.* **1995**, *103*, 6104.
- McGrath, M. P.; Radom, L. *J. Chem. Phys.* **1991**, *94*, 511.
- Watras, M. J.; Teplakov, A. V. *J. Phys. Chem. B* **2005**, *109* (18), 8928–8934.
- Dmitrenko, O.; Huang, W.; Polenova, T. E.; Francesconi, L. C.; Wingrave, J. A.; Teplakov, A. V. *J. Phys. Chem. B* **2003**, *107*, 7747–7752.
- Frantz, P.; Didziulis, S. V.; Fernandez-Torres, L. C.; Guenard, R. L.; Perry, S. S. *J. Phys. Chem. B* **2002**, *106*, 6456–6464.
- Cabanas, A.; Blackburn, J. M.; Watkins, J. J. *Microelectron. Eng.* **2002**, *64* (1–4), 53–61.
- Redhead, P. A. *Vacuum* **1962**, *12*, 203–211.
- Lebedev, B. V.; Lebedev, N. K.; Khotimskii, V. S.; Durgar'yan, S. G.; Nametkin, N. S. *Dokl. Akad. Nauk SSSR* **1981**, *259*, 629.
- Voronkov, M. G.; Baryshok, V. P.; Klyuchnikov, V. A.; Danilova, T. F.; Pepekina, V. I.; Korchagina, A. N.; Khudobin, Y. I. *J. Organomet. Chem.* **1988**, *345*, 27–38.
- Bocharov, S.; Mathauser, A. T.; Teplakov, A. V. *J. Phys. Chem. B* **2003**, *107*, 7776–7782.
- Bocharov, S.; Teplakov, A. V. *Surf. Sci.* **2004**, *573*, 403–412.
- Toth, L. E. *Transition Metal Carbides and Nitrides*; Academic Press: New York, 1971.
- Levy, R. L.; Boudart, M. *Science* **1973**, *181*, 547.
- Oyama, S. T. *The Chemistry of Transition Metal Carbides and Nitrides*; Blackie Academic and Professional: Glasgow, U.K., 1996.
- Chen, J. G. *Surf. Sci. Rep.* **1997**, *30* (1/3), 1–152.
- Fix, R. M.; Gordon, R. G.; Hoffman, D. M. *Chem. Mater.* **1990**, *2*, 235–241.
- Paserba, K. R.; Gellman, A. J. *Phys. Rev. Lett.* **2001**, *86* (19), 4338–41.
- Paserba, K. R.; Gellman, A. J. *J. Chem. Phys.* **2001**, *115* (14), 6737–51.
- Müller, T.; Flynn, G. W.; Mathauser, A. T.; Teplakov, A. V. *Langmuir* **2003**, *19*, 2812–2821.
- Ni, C.; Wells, M.; Zhang, Z.; Beebe, T. P., Jr.; Pirulli, L.; Méndez De Leo, L. P.; Teplakov, A. V., in preparation.
- Liu, P.; Rodriguez, J. A.; Muckerman, J. T. *J. Phys. Chem. B* **2004**, *108*, 18796–18798.
- Liu, P.; Rodriguez, J. A.; Muckerman, J. T. *J. Mol. Catal. A: Chem.* **2005**, *239*, 116–124.